ISSN : 0974 - 7451 Volume 8 Issue 5

Environmental Science
An Indian Journal
Current Research Paper

ESAIJ, 8(5), 2013 [186-191]

# Development and application of histidine-modified silica materials for Pb (II) removal from aqueous solutions

**Sanaa Saoiabi, Sanae El Asri, Abdelaziz. Laghzizil*, Ahmed Saoiabi**
**Laboratoire de Chimie Physique Générale, Faculté des Sciences, Université Mohamed V-Agdal, BP.1014, Rabat, (MOROCCO)**
**E-mail : laghzizi@fsr.ac.ma**

## ABSTRACT

Incorporation of histidine within silica was performed using the sol-gel process. The porosity of the materials decreases with organic content whereas its affinity for lead ions increases. The sorption kinetics and isotherms were studied, together with the variation of pH during the sorption reaction. These results indicate that the grafting histidine on porous silica presents synergy in the ability to complex Pb (II) ions, so the grafted histidine –silica can be employed as potential agent for lead remediation.


## KEYWORDS

Silica;
Histidine;
Hybrid materials;
Lead;
Remediation.

## INTRODUCTION

A significant current trend in new materials developments is the surface modification of usual supports to produce new and low-cost sorbents with well-defined surface characteristics, chemical and thermal stability[1-4]. Among of them, silica gels and their derivatives are well-known for their chromatographic applications[1]. In order to increase silica affinity for metal cations, a wide variety of organic molecules having basic centers such as sulfur, nitrogen and oxygen atoms, were grafted on the surface of porous silica[5-7]. However, the grafting procedure can be tedious, often involving the preparation of a functional silane or a two-step reaction based on the pre-functionalization of the silica surface[8-9]. As an alternative, the physical immobilization of organic molecules within silica gels via the sol-gel process can envisioned[10-11]. However, the pore size of silica gels often overpass the dimensions of small organics, resulting in rapid leaching of the encapsulated molecule, except if significant interactions exist with the silica surface[12]. Then, the porous modified silica materials with various chelating agents are increasingly utilized as adsorbents because of the high selectivity of the agents for metal ions adsorption[13-18]. Histidine is one of the strongest chelating ligands among the amino and carboxylic acids and plays an important role in the binding of metal ions in polluted water[19-21]. In this work, based on the reported ability of basic amino acids to interact strongly with silica, we have studied the possibility to obtain silica-histidine hybrid materials by simple incorporation of the organic precursor in the silica precursor solution. The influence of histidine content on the materials formation, composition and structure was studied. The performance of the hybrid materials for heavy metal immobilization was evaluated by studying

the sorption kinetics and isotherms of lead (II) ions. A mechanism for lead sorption was proposed based on data modeling together with the monitoring of pH variation during the sorption reaction.

## EXPERIMENTAL SECTION

### Sorbent synthesis

All chemical reagents were purchased from Aldrich. The pure silica materials were prepared by mixing 10.4 g of TEOS with 2.5 mL of water and 20 mL of ethanol under stirring and adjusting the pH to 2 using HCl. After 3 h of hydrolysis, the stirring was stopped and the condensation was left to proceed at room temperature for 24 h. The histidine-modified silica powders were obtained by adding 0.25 mol (SiH025) and 0.5 moles (SiH05) of histidine per mole of TEOS, previously dissolved in water, to the TEOS-water-ethanol solution. It was found necessary to heat the pre-hydrolyzed mixture at 40°C for 12 h and to keep it aging for 24 h at room temperature before gel formation. Attempts to use higher histidine content led to inhomogeneous gels. Silica and hybrid powders were obtained by placing the gels at 100°C overnight.

### Lead sorption experiments and modeling

A set of adsorption experiments were performed by dispersing 200 mg of powder materials in 100 mL of Pb $(NO_3)_2$ solution (concentration varying from 0.05 to 2.5 mmol.L$^{-1}$) at 25°C using a mechanical stirrer (EUROSTAR digital IKA) to provide reproducible and homogeneous mixing. The initial pH was adjusted to pH 5 and the variation of the pH of the lead solutions during metal adsorption was monitored. Experimental variations were in a 2% range. Lead sorption kinetics were measured by the same procedure but using 200 mL of lead solution (1.5 mmol.L$^{-1}$) with 400 mg of sorbent. Aliquots of the supernatant solution were taken with a 2 mL propylene syringe equipped with a 0.45 μm filter. All measurements were performed in triplicate and experimental errors were found below 5%. The residuel $Pb^{2+}$ into solution was chemically analyzed by inductively coupled plasma (ICP) emission spectroscopy (ICPS-7500, Shimadzu, Japan) and its concentration was calculated by using Eq.(1):

$$q(t) = \frac{C_0 - C_e(t)}{m} V \quad (1)$$

where q (t) is the amount (mmol.g$^{-1}$) of adsorbed lead (II), $C_0$ and $C_e$ are the initial and equilibrium concentrations (mmol.L$^{-1}$) in solution, V is the volume (L) of contaminated solution and m is the weight (g) of the adsorbent.

### Kenetics and isotherms

In order to determine the sorption rate constant, the Lagergren pseudo-first order model was applied to the experimental data[22]. The corresponding equation can be expressed as (eq. 2):

$$\log(q_e - q_t) = \log q_e - \frac{k}{2.303} t \quad (2)$$

where $q_e$ is the amount of adsorbed lead per gram of adsorbent (in mmol.g$^{-1}$) at equilibrium, and $k$ is the pseudo-first order rate constant (in min$^{-1}$).

The pseudo-second order model can be expressed as a differential equation[22]:

$$\frac{t}{q_t} = \frac{1}{k_2 q_{e,2}^2} + \frac{1}{q_{e,2}} t \quad (3)$$

The plot of $t/q_t$ against time $t$ of Eq. (3) should give a linear relationship from which the constants $q_{e,2}$ and $k_2$ can be determined from the intercept and slope of the plot.

Langmuir and Freundlich models are commonly used to study sorption processes [23]. The Langmuir adsorption model is based on the assumption that a maximum uptake exists, corresponding to a saturated monolayer of sorbed molecules on the adsorbent surface. The Langmuir equation can be written as:

$$\frac{C_e}{q_e} = \frac{1}{b.q_{\max}} + \frac{C_e}{q_{\max}} \quad (4)$$

where $q_e$ and $C_e$ are the equilibrium Pb (II) ions concentration on the adsorbent (mmol.g$^{-1}$) and in solution respectively (mmol.L$^{-1}$). The $q_{max}$ is the maximum uptake per unit mass of adsorbent (mmol.g$^{-1}$), and $b$ is the Langmuir constant related to the adsorption energy (L.mmol$^{-1}$)

The Freundlich adsorption model is more adapted to heterogeneous surface through a multilayer adsorption mechanism according to (eq. 5):

$$\log q_e = \log K_f + \frac{1}{n} \log C_e \quad (5)$$

where $C_e$ and $q_e$ have the same meaning as in the Langmuir isotherm, $K_F$ is the equilibrium constant of the adsorption reaction and *1/n* is the empirical parameter related to the intensity of adsorption, which varies with the heterogeneity of the material. When values are from 0.1 to 1, the adsorption conditions are favorable. The fitting procedure of kinetics and isotherm data was performed using the Kaleidagraph software that provide coefficient of determination $R^2$.

## Techniques

Powders were identified using a FTIR Nicolet Magna-IR 550 spectrophotometer from 4000 to 400 $cm^{-1}$. Thermogravimetry analysis (TGA) was carried out in airflow using a TA Instruments Netzsch STA-409EP apparatus. The thermal measurements were conducted from 30°C to 1000°C with 10°C/min as heating rate. The $N_2$ adsorption-desorption isotherms for dried powders were obtained by multi-point $N_2$ gas sorption experiments at 77 K using a Micromeritics ASAP 2010 instrument. The specific surface area was calculated according to the Brunauer–Emmett–Teller (BET) method using adsorption data in the relative pressure range from 0.05 to 0.25.

## RESULTS AND DISCUSSION

### Material characterization

The incorporation of histidine molecules within the silica network was first checked using thermogravimetric analyses (Figure 1). Taking the pure silica material as a reference, the weight loss in the 150°C-700°C range could be attributed to the decomposition of histidine moieties (TABLE 1) and the decomposed organic content increases with loss the histidine content. Characteristic bands of the histidine ring could be observed on FTIR spectra of SiH05, at 1560, 1505, and 1390 $cm^{-1}$, corresponding to N–C, C=C, and C–N=C stretching frequencies, respectively (Figure 2). Other main signals were attributed to the silica network: 1090 $cm^{-1}$ (triplet corresponding to Si-O stretching), 950 $cm^{-1}$ (Si-OH vibration mode), 800 $cm^{-1}$ (Si-O-Si bending) and 470 $cm^{-1}$ (Si-O bending). However, the presence of grafted histidine in silica matrix by forming the hydrogen or nitrogen bonding can explain the displacement the Si-O bands to the lower frequencies. The $N_2$-ad-

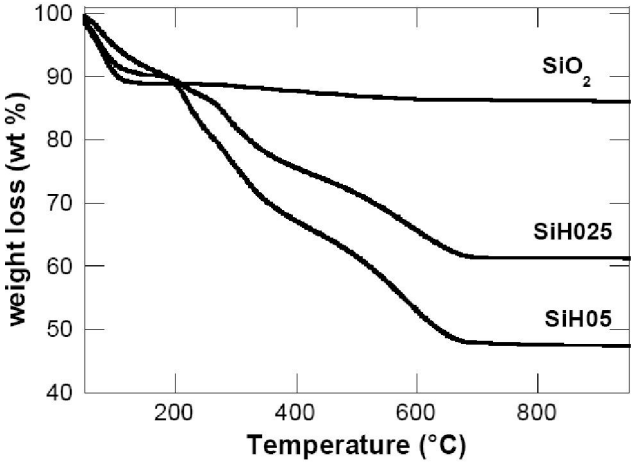


**Figure 1 : Thermogravimetric analysis of silica and silica-histidine hybrids.**

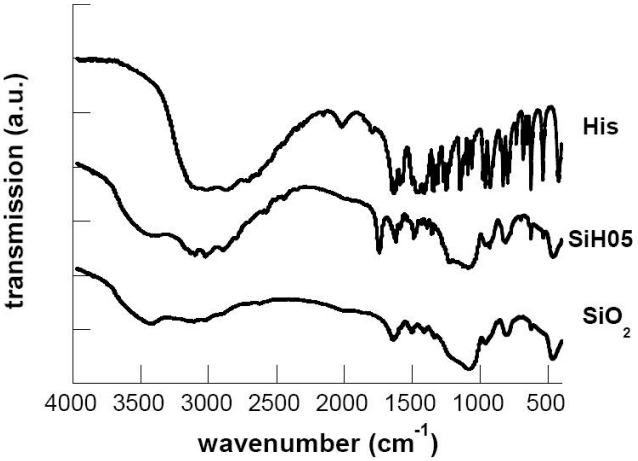


**Figure 2 : IR spectra of pure silica and histidine and SiH05 hybrid.**

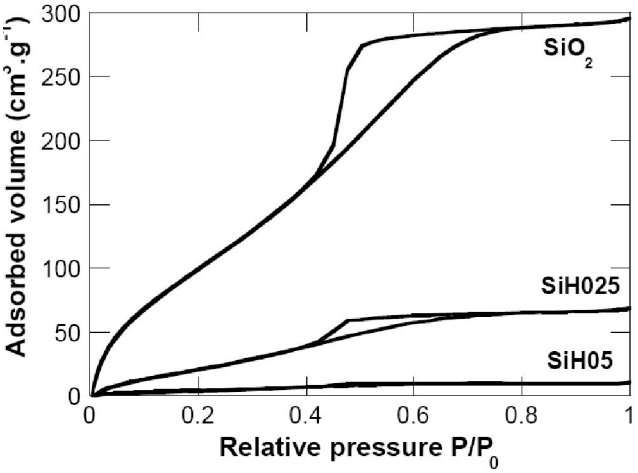


**Figure 3 : $N_2$-sorption isotherms of silica and silica-histidine hybrids**

sorption/desorption isotherms indicate that the micro- and mesoporous network of the pure silica material undergoes a marked decrease in specific surface area and porous volume of the silica network with increasing histidine content (Figure 3, TABLE 1). Altogether, these analyses indicate the successful incorporation of histidine in the porosity of the silica network.

**TABLE 1 : Organic content (wt%), specific surface area ($S_{BET}$), diameter pore ($D_p$), porous volume ($V_p$), experimental maximum capacity ($q_{max}$).**

| | | $SiO_2$ | SiH025 | SiH05 |
|---|---|---|---|---|
| Organic content | (wt%) | 0 | 32 | 45 |
| Specific surface area | $S_{BET}$ ($m^2.g^{-1}$) | 700 | 160 | 26 |
| Porous volume | $V_p$ ($cm^3.g^{-1}$) | 0.51 | 0.12 | 0.02 |
| Diameter pore | $D_p$ (nm) | 1.5 | 2.1 | 3.2 |
| Experimental adsorption capacity | $q_{exp}$(mmol.$g^{-1}$) | 0.07 | 0.44 | 0.65 |

## Adsorption studies: kinetics and isotherms

In the first part, kinetic experiments were performed using 1.5 mmol $L^{-1}$ as initial concentration. The kinetics of lead depletion from aqueous solution by silica and hybrid materials showed that sorption equilibrium was reached after 60 min for all materials (Figure 4). As shown in Figure 4, the presence of histidine in silica speed up the sorption process, but no significant effect of the equilibrium. When the two systems SiH025 and SiH05 are compared to the unmodified silica, the histidine-modification appears more efficient in enhancing the sorption rate. Attempts to plot log ($q_e$-$q_t$) against t for the pseudo-first-order equation were unsatisfactory especially for hybrid materials (SiH025 and SiH05) (Figure 4 and TABLE 2). It was noticed that non-linear plots were observed at the beginning of the adsorption process for hybrid adsorbents. As a result, correlation coefficients are poor (TABLE 2) so that calculated equilibrium sorption capacities, $q_{e,1}$ were not in accordance with the experimental results. However, the pseudo second order model (t/$q_t$ against t) reveals suitable to reproduce the experimental data ($R^2_{kin}$ >0.998). Extracted parameters from the both kinetic models are also gathered in TABLE 2. They show that, in these conditions, the lead sorption capacity at equilibrium $q_e$ depends of chemical surface modification, but that the sorption rate $k$ varied in the presence of histidine. The calculated equilibrium sorption capacities are 0.067 mmol $g^{-1}$, 0.429 mmol.$g^{-1}$ and 0.667 mmol.$g^{-1}$ for pure silica, SiH025 and SiH05, respectively. In parallel, the values of the rate constant, $k_2$, were found to be 1.484 mmol.$min^{-1}$, 0.339 mmol.$min^{-1}$ and 0.336 mmol.$min^{-1}$ for pure silica, SiH025 and SiH05, respectively, suggesting that the increase of the histidine content in silica network activates the $Pb^{2+}$ retention by complexation reactions. Consequently, the surface characteristics ($S_{BET}$, $V_p$, and $D_p$) were not main criteria in this adsorption process. Therefore, the second order model is in good agreement with experimental data. Sorption isotherms were determined on this basis of kinetic results especially on the equilibrium sorption time (Figure 5). Experimental maximum sorption capacity, $q_{e,max}$ increased with histidine content (TABLE 2). The experimental data on the effect of an initial concentration of $Pb^{2+}$ ions on the affinity of histidine-modified silicas were fitted to the isotherm models using Langmuir and Freundlich models to simulate the sorption isotherms. The Langmuir model was found well adapted to model the sorption data, with $R^2$ values close to unity (TABLE 2), and good agreement between the calculated curve and the experimental data (Figure 5). Langmuir constant $K_L$ was not significantly modified by histidine incorporation. The evolution of the pH of powder suspension in contact with acidified water containing no lead ions was first monitored (Figure 6). In these conditions, the pH dropped rapidly within 30 min and then more slowly, reaching equilibrium after ca. 2 hrs. Noticeably the equilibrium pH decreased with increasing histidine content. When $Pb^{2+}$ ions were present, a similar trend was observed, with final equilibrium pH being systematically lower than in the absence of metal. The data indicate that the incorporation of histidine significantly increases the affinity of the silica network for lead ions. Noticeably, such an increase cannot be attributed to an increase in accessible surface as $S_{BET}$ decreases from $SiO_2$ to SiH05. Therefore, it suggests that histidine provides additional binding sites for $Pb^{2+}$ on the silica surface. Interestingly, the successful fitting of isotherms using the Langmuir model indicates that lead ions consider the hybrid materials as a homogeneous surface, containing carboxylate and amine functions as chelating agents. Given the typical chemical surface of hybrid materials, it may be difficult to differentiate the both process adsorption/complexation and

this was observed on the same $K_L$ values for hybrid materials. Hydrated silica having an isoelectric point of *ca*. 3, it tends to release proton at pH 5, as observed here. Histidine has three acidic groups of $pK_a$ 2.4 (carboxylic acid) 6.0 (pyrole NH) and 9.2 (ammonium NH)[24-25]. Hence, deprotonation of the carboxylic acid function may occur at the same pH. The interaction of lead ions with the silica surface should further favor deprotonation of silanol to silanolate. These results implied that lead adsorption seemed to progress by ion-exchange with carboxylic groups. Accordingly, in addition to favorable electrostatic interactions with carboxylate functions, $Pb^{2+}$ may also interact with the pyrrole amine groups, favoring their deprotonation. Finally, it is important to note that sorption capacity of SiH05 towards $Pb^{2+}$ is among the highest reported so far for silica-modified materials obtained by surface grafting[26-28].

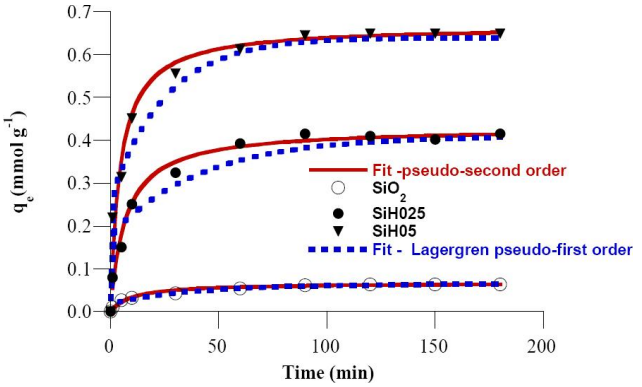


**Figure 4 : Effect of incubation time on $Pb^{2+}$ adsorption $q_t$ onto histidin grafted silica with varying histidin content. ($C_0$ = 1.5 mmol/L, pH=5, dose=2g.L$^{-1}$).**

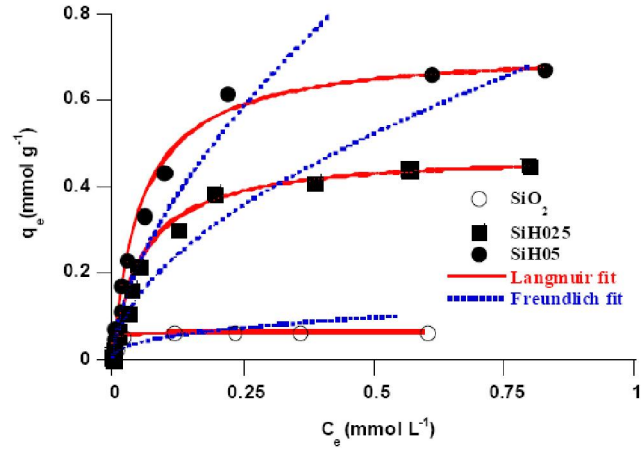


**Figure 5 : Variation of sorbed $Pb^{2+}$ ($q_e$) with metal concentration $C_e$ at equilibrium onto silica and silica-**

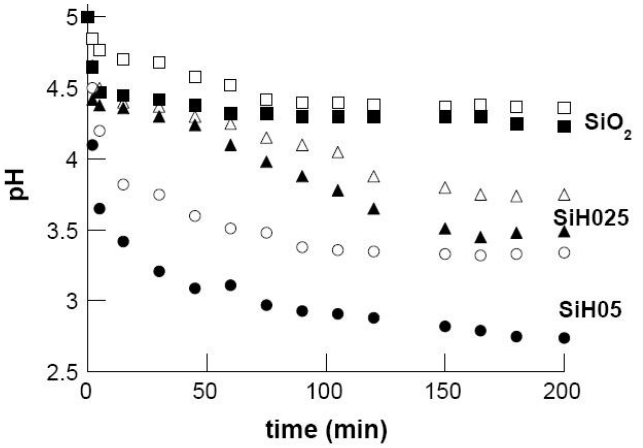


**Figure 6. pH evolution of acidified water (pH 5, open symbols) and added 1.5 mmol L-1 Pb2+ (plain symbols) in presence of silica and histidine-silica materials.**

**TABLE 2 : Kinetic and Isotherm fit parameters for the adsorption of $Pb^{2+}$ onto histidine modified silica sorbents.**

| | | | $SiO_2$ | SiH025 | SiH05 |
|---|---|---|---|---|---|
| Kinetic models | Experimental | $q_e$ (mmol.g$^{-1}$) | 0.064 | 0.412 | 0.658 |
| | First order | $q_{e,1}$ (mmol.g$^{-1}$) | 0.053 | 0.230 | 0.480 |
| | | $k_1$ (min$^{-1}$) | 0,033 | 0,026 | 0,051 |
| | | $R^2$ | 0.9411 | 0.9232 | 0.9527 |
| | Second order | $q_{e,2}$ (mmol.g$^{-1}$) | 0.067 | 0.429 | 0.667 |
| | | $k_2$ (mmol.min$^{-1}$) | 1.484 | 0.339 | 0.336 |
| | | $R^2$ | 0.9985 | 0.9993 | 0.9998 |
| Isotherms | Experimental | $q_e$ (mmol.g$^{-1}$) | 0.07 | 0.44 | 0.65 |
| | Langmuir | $q_{e,max}$ (mmol.g$^{-1}$) | 0.06 | 0.48 | 0.70 |
| | | $K_L$ (g.mmol$^{-1}$) | 23 | 18 | 17 |
| | | $R^2$ | 0.999 | 0.997 | 0.999 |
| | Freundlich | 1/n | 0.406 | 0.552 | 0.609 |
| | | $K_F$ | 0.123 | 0.765 | 1.357 |
| | | $R^2$ | 0.9702 | 0.9852 | 0.9702 |

## CONCLUSION

The one-step incorporation of histidine within silica gels allowed the formation of homogeneous hybrid materials. Although our approach is much simpler than reported grafting approaches, these materials exhibit some of the highest sorption capacity reported so far. This can be attributed to the high amount of organic ligand that can be immobilized by this method. Indeed, its main drawback relies in the possible loss of binding capacity upon recycling due to weaker interactions between histidine and silica compared to covalently grafted ligands.

This point will be investigated in a near future.

## REFERENCES


**[1]** J.E.Schiele, R.Mallik, S.Soman, K.S.Joseph, D.S.Hage; J.Sep.Sc., **29**, 719-737 **(2006)**.

**[2]** A.R.Cestari, C.Airoldi; J.Colloid Interface Science, **195**, 338-342 **(1997)**.

**[3]** H.Rhaiti, A.Laghzizil, A.Saoiabi, S.El Asri, K.Lahlil, T.Gacoin; Materials Chemistry and Physics, **136**, 1022-1026 **(2012)**.

**[4]** H.Bouyarmane, S.El Asri, A.Rami, C.Roux, M.A.Mahly, A.Saoiabi, T.Coradin, A.Laghzizil, J.Hazard.Mat., **181**, 736-741 **(2010)**.

**[5]** F.A.Pavan, I.S.Lima, E.V.Benvenutti, Y.Gushikem, C.Airoldi; J.Colloid Interf.Sci., **275**, 386-391 **(2004)**.

**[6]** L.N.H.Arakaki, V.L.S.Augusto-Filha, K.S.Sousa, F.P.Aguiar, M.G.Fonseca, J.G.P.Espinola; Thermochimica Acta ,**440,** 176-180 **(2006)**.

**[7]** D.V.Quang, J.K.Kim, P.B.Sarawade, D.H.Tuan; Hee Taik Kim, J.Ind.Eng.Chem., **18**, 83-87 **(2012)**.

**[8]** K.Kusakabe, S.Sakamoto, T.Saie, S.Morooka; Sep.Pur.Technol., **16**, 139-146 **(1999)**.

**[9]** M.Pagliaro, R.Ciriminna, G.Palmsano; Chem.Soc.Rev., **36**, 932-40 **(2007)**.

**[10]** A.G.S.Prado, J.A.A.Sales, R.M.Carvalho, J.C.Rubin, C.Airoldi; Journal of Non-Crystalline Solids, **333**, 61-67 **(2004)**.

**[11]** C.E.Fowler, C.Buchber, B.Lebeau, J.Patarin, C.Delacote, A.Walcarius; Applied Surface Science, **253,** 5485-5493 **(2007)**.

**[12]** T.Coradin, J.Livage; Colloids and Surfaces B: Biointerfaces, **21**, 329-336 **(2001)**.

**[13]** R.Rostamian, M.Najafic, A.A.Rafati; Chemi.Eng. J., **171,** 1004-1011 **(2011)**.

**[14]** M.Najafi, R.Rostamian, A.A.Rafati; Chem.Eng.J., **168**, 426-432 **(2011)**.

**[15]** H.T.Fan, T.Sun, H.B.Xu, Y.J.Yang, Q.Tang, Y.Sun; Desalination, **278**, 238-243 **(2011)**.

**[16]** M.Najafi, Y.Yousefi, A.A.Rafati; Sep.Pur.Technol., **85**, 193-205 **(2012)**.

**[17]** J.S.Kim, J.Yi; Sep.Sci.Technol., **34**, 2957-2971 **(1999)**.

**[18]** N.Chiron, R.Guilet, E.Deydier; Water Research, **37**, 3079-86 **(2003)**.

**[19]** S.Saoiabi, S.El Asri, A.Laghzizil, A.Saoiabi, J.L.Ackerman, T.Coradin; Chemical Engineering Journal, **211-212**, 233-239 **(2012)**.

**[19]** Tse-Shien Chen, Chuen-Ying Liu; Electrophoresis, **22**, 2606-2615 **(2001)**.

**[21]** M.Louloudi, Y.Deligiannakis, N.Hadjiliadis; Inorg.Chem., **37**, 6847-6851 **(1998)**.

**[22]** Y.S.Ho, J.Hazard; Mater., **136**, 681-689 **(2006)**.

**[23]** I.Langmuir; J.Am.Chem.Soc., **40**, 1361-1403 **(1918)**.

**[24]** P.Deschamps, P.P.Kulkarni, M.Gautam-Basak, and B.Sarkar; Coordination Chemistry Reviews, **249**, 895-909 **(2005)**.

**[25]** C.Guo Nan, W.Xiao Ping, D.Jian Ping, and C.Hong Qing; Talanta, **49**, 319-330 **(1999)**.

**[26]** M.Rasouli, N.Yaghobi, M.Hafezi, M.Rasoul, J.Ind.Eng.Chem., **18**, 1970-1976 **(2012)**.

**[27]** F.A.Pavan, T.M.H.Costa, V.Edilson, E.V.Benvenutti; Colloids Surf A, **226**, 95-100 **(2003)**.

**[28]** H.T.Barcelos, L.D.Nunes, G.W.Tavares, E.F.C.Alcantara, A.G.S.Prado; J.Therm.Calorim., **106**, 421-425 **(2011)**.